BIOCHEMISTRY
including biophysical chemistry & molecular biology

RAPID REPORT

pubs.acs.org/biochemistry

A Combinatorial Approach to Engineering a Dual-Specific Metal Switch Antibody

Sean W. Fanning,[†] Megan L. Murtaugh,[†] and James R. Horn[*,†,‡]

[†]Department of Chemistry and Biochemistry and [‡]Center for Biochemical and Biophysical Studies, Northern Illinois University, DeKalb, Illinois 60115, United States

Supporting Information

ABSTRACT: There is considerable interest in understanding how multiple binding events can be mediated through a single protein interface. Here, a synthetic library approach was developed to generate a novel dual-specific antibody. Using a combinatorial histidine-scanning phage display library, potential metal binding sites were introduced throughout an anti-RNase A antibody interface. Stepwise selection of RNase A and metal binding produced a dual-specific antibody that retained near wild-type affinity for its target antigen while acquiring a competitive metal binding site that is capable of controlling the antibody−antigen interaction. Structure analysis of the original antibody−RNase A complex suggested peripheral interface residues and loop flexibility are key contributors for obtaining the dual specificity.

Biology employs a number of strategies to regulate protein binding events (e.g., oligomerization and protein allostery); however, the underlying principle behind most regulation is simply linked equilibria. A minimalist example of such linked-equilibria-based regulation involves a single (common) protein interface that is capable of recognizing more than one target. Such promiscuous protein binding can serve to enhance or preclude secondary binding events and frequently plays a role in regulating signaling pathways.[1] In general, the underlying structural properties of such dual-specific protein interfaces are not well understood as the types of interactions that are necessary for each binding event may be significantly different.

Metal binding proteins are among the most commonly observed dual-specific proteins. Metal binding sites play roles in events such as substrate recognition and binding site stabilization. Consequently, there has been considerable interest and success in developing novel protein metallorecognition sites.[2,3] In particular, histidine side chains play a prominent role in metal binding sites and can bind metal ions (e.g., nickel, zinc, and cobalt) with as few as two histidine side chain groups. Such bi-histidine sites have been engineered to regulate enzyme activity,[4] examine folding,[5] and enhance protein stability.[6] Whether the metal binding site is physiological or engineered, metal coordination and protein scaffolding play an essential role in determining the protein's affinity for metal ions. Consequently, traditional efforts to design novel metal binding sites rely heavily on knowledge of the protein's three-dimensional structure. Furthermore, most design efforts introduce metal binding sites within rigid protein scaffolding, such as helices[5] or at the interface of oligomeric states of helical bundle proteins[7,8] and not typically within loop regions.

On the basis of the frequently observed "plastic" nature of protein−protein interfaces, where many interface residues can tolerate substitutions without a significant loss of binding affinity,[9−11] we explore the hypothesis that such interface residues could be designed to possess new function (i.e., metal binding), without the loss of the original function (i.e., protein binding). Specifically, using a novel, library-based technique, we sought to introduce a competitive metal binding site within the CDR loops of a model antibody−antigen interface. The engineered dual specificity would thereby serve as a metal switch that could modulate the antibody−antigen interaction through the presence of metal ions. Figure 1A depicts the underlying linked-equilibria model, where K_{int} and K_{metal} are the antigen and metal binding equilibrium constants, respectively. Antibody recognition of the two targets, antigen and metal, is mutually exclusive, which results in an overall observed antigen binding constant, K_{obs}, that is dependent on metal concentration.

A combinatorial approach was developed that would (1) "saturate" the antibody interface with metal binding ligands and (2) allow the retention of residues that are energetically critical to RNase A binding. This approach, termed combinatorial histidine scanning, screened 22 residue positions within the antigen binding interface of anti-RNase A VHH.[13] Using degenerate oligonucleotide-directed mutagenesis,[14] each residue position was allowed to sample the original wild-type residue and histidine (Figure 1B). Consequently, every possible combination of histidine and wild-type residue was sampled throughout the interface. This corresponds to 2^{22} (or 4×10^6) unique His/wild-type variants. The histidine-scanning anti-RNase A VHH library was then displayed on the surface of M13 phage and subjected to a coselection strategy (Supporting Information). To maintain the anti-RNase A VHH's high affinity ($K_d \sim 20$ nM), the first round of phage panning selected variants that solely recognized RNase A. Over the next three rounds of selection, VHH-presenting phage were initially selected for RNase A binding, followed by competitive selection of metal sensitive VHH clones using a metal ion mixture (i.e., cobalt, nickel, and zinc). To increase the stringency of selection of binding both RNase A and metal, the concentrations of VHH and metal were decreased each round. After four total rounds of selection, immunoassay screening allowed identification of a metal sensitive anti-RNase A

Received: March 15, 2011
Revised: May 6, 2011
Published: May 13, 2011

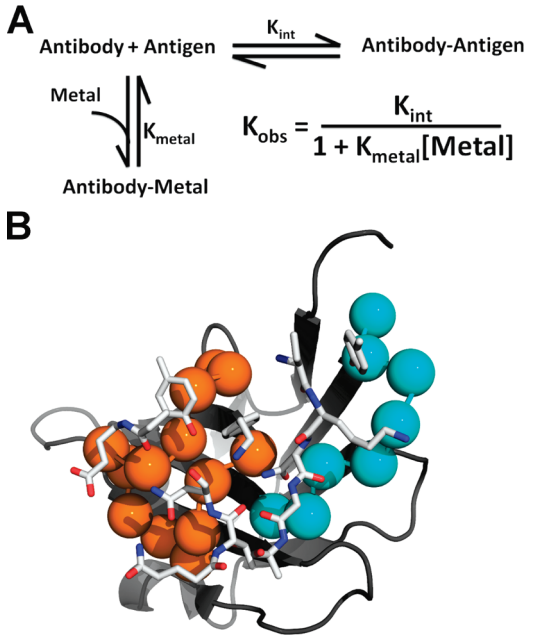

Figure 1. (A) Linked-equilibria model for a dual-binding anti-RNase A VHH. (B) Interface view of the 22 positions included in the combinatorial histidine/wild-type library: CDR1 (cyan), CDR3 (orange), and RNase A (white sticks).

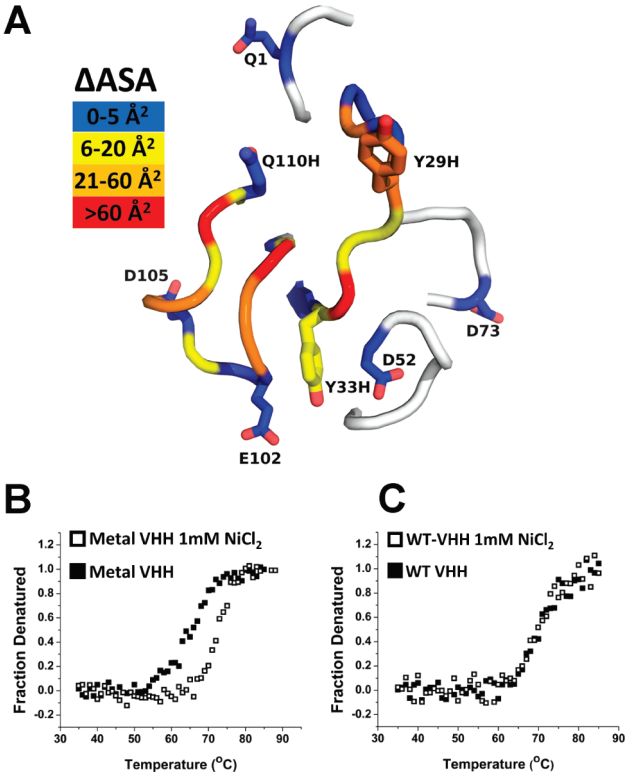

Figure 2. (A) Interface view of anti-RNase A VHH. Potential metal binding residues are shown as sticks. Positions are color-coded according to the change in accessible surface area upon binding RNase A. Values based on the wild-type anti-RNase A VHH−RNase A complex structure.[12] (B and C) Thermal unfolding of the VHH-metal variant and wild-type anti-RNase A, respectively, with and without 1 mM Ni^{2+}.

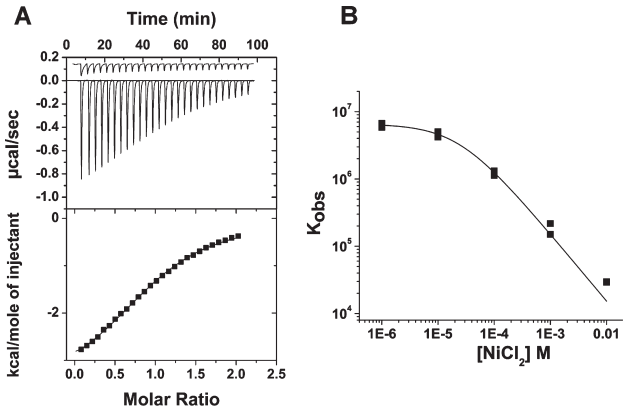

Figure 3. (A) ITC titration of nickel into the metal binding VHH-metal (200 μM). Dilution heats are offset in the top panel. (B) Observed binding constant for VHH-metal as a function of nickel concentration.

VHH clone. This clone, VHH-metal, possessed three histidine substitutions, Y29H, Y33H, and Q110H (Figure 2A).

To examine VHH-metal's specificity, circular dichroism (CD) was used to monitor thermal stability in the absence or presence of each metal (1 mM) used during screening (i.e., cobalt, nickel, and zinc). An increase in the melting temperature, T_m, of approximately 7 °C was observed in the presence of 1 mM nickel (Figure 2B), whereas smaller shifts in T_m were observed in the presence of either zinc or cobalt. Consequently, nickel was used for all subsequent experiments. Control experiments revealed the thermal stability of the wild-type anti-RNase A VHH was unchanged in the presence and absence of 1 mM nickel (Figure 2C), indicating the nickel binding was due to the remodeled interface. Similarly, control experiments with the antigen, RNase A, with and without metal, displayed no change in T_m (data not shown). Comparison of the thermal unfolding of VHH-metal to the original anti-RNase VHH, in the absence of metal, revealed that the remodeled metal interface resulted in a decrease in T_m by ~4 °C (Figure 2B,C).

Isothermal titration calorimetry (ITC) was used to evaluate the thermodynamic basis for VHH-metal's dual function. Figure 3A displays titrations of nickel into VHH-metal, which revealed a metal binding dissociation constant, K_d, of 30 ± 10 μM. This value is comparable to affinities reported for other nickel binding proteins.[15] As expected, titrations of nickel into wild-type anti-RNase A VHH produced no measurable binding. In the absence of metal, VHH-metal possessed a slightly decreased binding affinity for RNase A (K_d = 155 ± 5 nM) compared to that of wild-type anti-RNaseA VHH (K_d = 19 ± 1 nM), which corresponds to an ~8-fold decrease in binding affinity ($\Delta\Delta G°$ = 1.2 kcal/mol). Overall, the thermodynamic basis for binding to RNase A did not dramatically change versus the wild-type anti-RNase A VHH, where recognition of RNase A is primarily based on a favorable enthalpic contribution overcoming an unfavorable entropic penalty (Supporting Information). To determine whether metal binding could compete with RNase A binding, VHH−RNase A binding was examined over a range of nickel ion concentrations (10 μM to 10 mM). As displayed in Figure 3, the observed binding constant, K_{obs}, is clearly influenced by the presence of increasing concentrations of nickel. Fitting the model (Figure 1A) to the data revealed a metal binding constant, K_{metal}, of (4.3 ± 0.8) × 10^4 (K_d = 23 ± 5 μM), which is within error of the metal

dx.doi.org/10.1021/bi2003845 |*Biochemistry* 2011, 50, 5093–5095

binding constant measured independently. Overall, this suggests that formation of the metal binding site must significantly perturb and/or block the RNase A binding site.

Existing knowledge of the wild-type anti-RNase A VHH–RNase A complex structure[12,13] helps provide insight into how the VHH interface may accommodate a metal binding site yet retain the ability to bind RNase A. Overall, the distances between the C_α atoms for the three inserted histidines, H29, H33, and H110, all fall between 11 and 14 Å. These distances are within commonly expected ranges for metal binding sites.[15] In addition, it is possible that residue(s) preexisting in the interface may contribute as metal ligands, e.g., Q1, D52, D73, E102, and D105 (see Figure 2A). Consequently, the engineered metal binding site is likely to use at least two histidines and may include preexisting residues. Of the three histidine substitutions, Y29H and Q110H are located in solvent accessible positions, while Y33H would be predicted to participate in significant intramolecular contacts at the C-terminal end of CDR1 (Figure 2A). Consequently, it is predicted that the Y33H substitution would be conformationally restricted in its ability to form a metal binding site, while Y29H and Q110H substitutions would be better posed to form a metal site. Finally, it is worth noting that the metal site is specific for nickel as titrations performed in the presence of calcium ions did not show any appreciable change in the observed binding constant (data not shown).

Perhaps the most interesting feature of the engineered metal binding complex is that it must induce significant structural change and/or steric restriction that is capable of prohibiting RNase A binding, while not adversely affecting RNase A binding in the absence of metal. Clearly, conformational flexibility of the CDRs appears to be advantageous for the acquired dual specificity. Furthermore, of the three substitution sites (Y29H, Q110H, and Y33H), two of the substituted residues are tyrosines. Such isosteric substitution may be common when acquiring dual-specific binding properties, as long as the replacement residues serve as useful "filler" residues. Also, all substituted His residues are located in peripheral positions. For instance, upon formation of the wild-type complex, only Y33 buries significant surface area (through van der Waals contacts). Future structural and biophysical studies will be necessary to investigate the role that specific residues and loop conformation play in metal binding affinity and specificity.

Overall, a combinatorial histidine-scanning library approach was developed that introduced a metal switch into an existing antibody interface with minimal effects on antigen target affinity. This approach is analogous to a combinatorial histidine scanning library approach that has been used successfully to insert proton binding sites within a VHH interface to engineer pH sensitive binding (M. L. Murtaugh and J. R. Horn, unpublished results). These combinatorial approaches are robust and do not require knowledge of the protein structure (other than knowledge of the binding loops). The resulting metal binding affinity was determined to be comparable to those of several previously engineered metal binding sites. However, unlike metal binding site design for engineering metal cofactors in catalytic antibodies,[16] regulating enzyme activity,[4] or enhancing protein stability,[6] here, the engineered metal binding site was capable of successfully inhibiting a protein–protein interaction. It is perhaps somewhat surprising that only a single metal binding VHH clone was identified. This may due to excessively stringent selection. Alternatively, it is likely that the introduction of additional interface metal ligands (e.g., Glu, Asp, etc.) may ultimately be necessary to develop higher-affinity metal binding sites. Such metal binding sites will provide new routes in which to modulate protein binding. Finally, these results, along with two other known multispecific antibodies,[17,18] may suggest antibody interfaces are ideally suited to acquiring multispecific target binding, whether naturally or engineered.

■ ASSOCIATED CONTENT

Supporting Information. Additional materials and methods, a figure, and tables of binding thermodynamics. This material is available free of charge via the Internet at http://pubs.acs.org.

■ AUTHOR INFORMATION

Corresponding Author

*E-mail: jrhorn@niu.edu. Telephone: (815) 753-8654. Fax: (815) 753-4802.

Funding Sources

This work was supported by National Science Foundation Grant MCB-0953323 to J.R.H.

■ REFERENCES

(1) Erijman, A., Aizner, Y., and Shifman, J. M. (2011) *Biochemistry 50*, 602–611.

(2) Lu, Y., Yeung, N., Sieracki, N., and Marshall, N. M. (2009) *Nature 460*, 855–862.

(3) Matthews, J. M., Loughlin, F. E., and Mackay, J. P. (2008) *Curr. Opin. Struct. Biol. 18*, 484–490.

(4) Higaki, J. N., Haymore, B. L., Chen, S., Fletterick, R. J., and Craik, C. S. (1990) *Biochemistry 29*, 8582–8586.

(5) Krantz, B. A., and Sosnick, T. R. (2001) *Nat. Struct. Biol. 8*, 1042–1047.

(6) Zhuang, S., Peng, Q., Cao, Y., and Li, H. (2009) *J. Mol. Biol. 390*, 820–829.

(7) Salgado, E. N., Ambroggio, X. I., Brodin, J. D., Lewis, R. A., Kuhlman, B., and Tezcan, F. A. (2010) *Proc. Natl. Acad. Sci. U.S.A. 107*, 1827–1832.

(8) Salgado, E. N., Faraone-Mennella, J., and Tezcan, F. A. (2007) *J. Am. Chem. Soc. 129*, 13374–13375.

(9) Gerstner, R. B., Carter, P., and Lowman, H. B. (2002) *J. Mol. Biol. 321*, 851–862.

(10) Kouadio, J. L., Horn, J. R., Pal, G., and Kossiakoff, A. A. (2005) *J. Biol. Chem. 280*, 25524–25532.

(11) Atwell, S., Ultsch, M., De Vos, A. M., and Wells, J. A. (1997) *Science 278*, 1125–1128.

(12) Koide, A., Tereshko, V., Uysal, S., Margalef, K., Kossiakoff, A. A., and Koide, S. (2007) *J. Mol. Biol. 373*, 941–953.

(13) Decanniere, K., Desmyter, A., Lauwereys, M., Ghahroudi, M. A., Muyldermans, S., and Wyns, L. (1999) *Structure 7*, 361–370.

(14) Sidhu, S. S., and Weiss, G. A. (2004) Constructing phage display libraries by oligonucleotide-directed mutagenesis. In *Phage Display: A practical approach* (Clackson, T., and Lowman, H. B., Eds.) pp 27–41, Oxford University Press, Oxford, U.K.

(15) Higaki, J. N., Fletterick, R. J., and Craik, C. S. (1992) *Trends Biochem. Sci. 17*, 100–104.

(16) Roberts, V. A., Iverson, B. L., Iverson, S. A., Benkovic, S. J., Lerner, R. A., Getzoff, E. D., and Tainer, J. A. (1990) *Proc. Natl. Acad. Sci. U.S.A. 87*, 6654–6658.

(17) James, L. C., Roversi, P., and Tawfik, D. S. (2003) *Science 299*, 1362–1367.

(18) Bostrom, J., Yu, S. F., Kan, D., Appleton, B. A., Lee, C. V., Billeci, K., Man, W., Peale, F., Ross, S., Wiesmann, C., and Fuh, G. (2009) *Science 323*, 1610–1614.